Am J Transl Res 2026;18(7):5612-5622
www.ajtr.org /ISSN:1943-8141/AJTR0170337

Original Article

Lipopolysaccharide promotes bladder cancer immunosuppression by disrupting the Tfh/Tfr balance through TLR4 signaling

Bo Peng[1*], Yan Wang[2*], Haochen Li[3*], Changshui Zhuang[4], Rijian Guan[4], Haopeng Zhang[5], Lijun Wan[4]

[1]Reproductive Medicine Center, The Quzhou Affiliated Hospital of Wenzhou Medical University, Quzhou People's Hospital, Quzhou, Zhejiang, China; [2]Department of Laboratory Animal Sciences, Tianjin Medical University, Tianjin, China; [3]Tianjin International Travel Health Care Center, Tianjin, China; [4]Department of Urology, The Quzhou Affiliated Hospital of Wenzhou Medical University, Quzhou People's Hospital, Quzhou, Zhejiang, China; [5]School of Medical Technology, Tianjin University of Traditional Chinese Medicine, Tianjin, China. [*]Co-first authors.

Received November 27, 2025; Accepted February 6, 2026; Epub July 15, 2026; Published July 30, 2026

Abstract: Objective: To investigate the role of lipopolysaccharide (LPS)-mediated toll-like receptor 4 (TLR4) signaling in modulating the tumor immune microenvironment, particularly the follicular helper T cell (Tfh)/follicular regulatory T cell (Tfr) equilibrium, in bladder cancer. Methods: MBT-2 and MB49 cells were treated with LPS. TLR4 was knocked down using lentiviral short hairpin RNA. Cell proliferation, migration, and invasion were assessed by methylthiazolyldiphenyl-tetrazolium bromide, scratch, and Transwell assays. A subcutaneous xenograft model in C57BL/6 and C3H/He mice was established. Tfh/Tfr cells in spleens were analyzed by flow cytometry. TLR4 and related cytokine expression were measured by quantitative polymerase chain reaction and western blot. Results: LPS treatment upregulated the expression of TLR4/myeloid differentiation primary response 88, which enhanced tumor cell proliferation and migration *in vitro* and promoted tumor growth *in vivo*. These pro-tumor effects were reversed by TLR4 knockdown. Furthermore, LPS skewed the Tfh/Tfr ratio in favor of Tfh cells. At the cytokine level, LPS increased the production of interleukin-21 but decreased the levels of forkhead box P3, interleukin-10, and transforming growth factor-beta. All these immunologic alterations were also abolished upon TLR4 knockdown. Conclusion: LPS exacerbated bladder cancer progression by activating TLR4 signaling. This disrupts the Tfh/Tfr balance and creates an immunosuppressive niche. Targeting this axis may represent a novel therapeutic strategy.

Keywords: Bladder cancer, lipopolysaccharide, toll-like receptor 4, T follicular helper cells, T follicular regulatory cells, immunosuppression

Introduction

Bladder cancer (BCa) represents one of the most prevalent malignancies of the urinary tract. BCa is characterized by high rates of recurrence and progression, which pose persistent challenges to clinical management [1]. Although immunotherapeutic strategies notably Bacillus Calmette-Guérin (BCG) intravesical instillation have achieved significant success, a substantial proportion of patients exhibit non-response or eventual relapse. This underscores the complexity of the tumor immune microenvironment (TIME) and the resilience of immune evasion mechanisms in BCa [2]. Consequently, elucidating the key mechanisms that drive immunosuppression within the TIME is crucial for developing novel therapeutic strategies and improving patient outcomes.

Toll-like receptor 4 (TLR4) is a pivotal pattern recognition receptor in the innate immune system. It recognizes primarily pathogen-associated molecular patterns such as lipopolysaccharide (LPS) [3]. In tumor biology, the TLR4 signaling pathway assumes a complex dual role. While its activation in immune cells can promote anti-tumor immunity, growing evidence indicates that aberrant TLR4 activation within tumor cells themselves directly enhances malignant behaviors - such as proliferation, migration, and metastasis - and fosters an immuno-

https://doi.org/10.62347/CQYQ8046

suppressive tumor microenvironment [4, 5]. In BCa, elevated TLR4 expression correlates with adverse pathologic features and may be linked to urinary tract infections - a known risk factor often involving LPS exposure [6, 7]. However, the precise mechanism by which the LPS/TLR4 axis remodels the anti-tumor immunity in BCa, particularly through regulating the functional balance of key immune cell subsets, remains unclear.

Follicular helper T (Tfh) cells and follicular regulatory T (Tfr) cells are two critical $CD4^+$ T cell subsets that have recently emerged as central regulators of humoral immunity, with opposing functions in governing germinal center reactions [8]. Functionally, Tfh cells promote B cell activation and antibody production by secreting cytokines like interleukin-21 (IL-21). In contrast, Tfr cells, which express forkhead box P3 (Foxp3) and cytotoxic T-lymphocyte-associated protein 4 among other markers, act to suppress Tfh cell activity and thereby restrain excessive antibody responses. Tfh/Tfr dynamic equilibrium is essential for immune homeostasis [9, 10]. Dysregulation of this balance in the TIME is closely associated with immune evasion. Nevertheless, whether and how LPS/TLR4 signaling drives BCa immunosuppression by influencing the Tfh/Tfr balance represents a significant knowledge gap.

This study aimed at systematically investigating the regulatory role of LPS, through the TLR4 pathway, in BCa progression and the TIME, with a specific focus on the Tfh/Tfr cell equilibrium as a novel perspective. Using a BCa model, our research demonstrated for the first time that exogenous LPS, through activating TLR4/myeloid differentiation primary response 88 (myD88) signaling, not only directly enhances tumor cell malignancy but also significantly skews the balance between Tfh and Tfr cells toward Tfh. This is coupled with the modulation of key cytokines, including IL-21, interleukin-10 (IL-10), and transforming growth factor-beta (TGF-β), collectively fostering an immunosuppressive niche favorable to tumor growth. These findings provide novel mechanistic insight into immune evasion in BCa, particularly under infection- or inflammation-associated conditions, and offer an important theoretical basis for targeting the TLR4 signaling axis or the Tfh/Tfr balance to enhance the efficacy of existing immunotherapies.

Materials and methods

Cell culture and grouping

In culture medium containing 10% fetal bovine serum (FBS), bladder cancer cell lines were maintained. For BCa studies, cell proliferation, migration, and apoptosis were assessed using MBT-2 (ATCC® CRL-1749™) and MB49 (ATCC® HTB-2™) cells. Upon reaching 85% confluence in culture dishes, cells were divided into three groups: control, control + LPS (Sigma-Aldrich, L2630), and knockdown (KD) + LPS.

To knock down TLR4, cells were transduced with lentiviruses encoding si-TLR4. Stable TLR4-KD cell lines were generated by subsequent culture in fresh medium containing FBS. Specifically, stable TLR4-KD was achieved by infecting cells with lentivirus carrying short hairpin RNA (shRNA) targeting human TLR4. The shRNA sequence targeting TLR4 was 5'-GCAACAAAGTCCTGAAAGA-3'. A scrambled shRNA sequence (5'-TTCTCCGAACGTGTCACGT-3') was used as a negative control. Lentiviral particles were produced by co-transfecting HEK293T cells with the packaging plasmids psPAX2 and pMD2.G. Cells were infected in the presence of 8 μg/mL polybrene and selected with 2 μg/mL puromycin for 7 days to establish stable KD lines (MBT-2-KD-TLR4 and MB49-KD-TLR4). KD efficiency was confirmed by quantitative polymerase chain reaction (qPCR) and western blot analysis.

Methylthiazolyldiphenyl-Tetrazolium Bromide (MTT) assay for cell growth

Cells from each group were trypsinized and seeded into 96-well plates for culture in a 37°C incubator with 5% CO_2. After 24 to 48 hours, the MTT solution (Dojindo Molecular Technologies, CK04) was added to each well. Following a 4-hour incubation, the formazan crystals were dissolved. The optical density at 450 nm was measured using a microplate reader to assess cell viability.

Transwell assay for cell migration

Cell migration was evaluated using 24-well Transwell chambers with 8-μm pores (Corning,

Table 1. Primer sequences used for quantitative real-time PCR

Gene	Type	Sequence (5'→3')	Product Size (bp)
TLR4	F	TCCCTGCATAGAGGTGTGAAA	160
	R	GTCTCCACAGCCACCAGATT	
MyD88	F	TGTTCTTGAACCCTCGGACG	241
	R	TTCTGGCAGTCCTCCTCGAT	
Foxp3	F	ATCCCCCTCTAGCAGTCCAC	229
	R	AGTTGCCGGGAGAGCTGAAT	
IL-10	F	ATGCAGGACTTTAAGGGTTACTT	255
	R	GTAGACACCTTGGTCTTGGAG	
IL-21	F	CCACAAGATGTAAAGGGGCAC	299
	R	GGTACCCGGACACAACATGG	
TGF-β	F	AGCTCCTCATCGTGTTGGTG	273
	R	TGCAGTGGTCCTGATTGCAG	
GAPDH	F	GTGGCAAAGTGGAGATTGTTG	99
	R	CGTTGAATTTGCCGTGAGTG	

Abbreviations: TLR4, Toll-like receptor 4; MyD88, Myeloid differentiation primary response 88; Foxp3, Forkhead box P3; IL-10, Interleukin-10; IL-21, Interleukin-21; TGF-21; TGF-response 88; Foxp3, Forkhead box P3; IL-10, Interleukin-10; e dehydrogenase; F, Forward primer; R, Reverse primer; bp, base pairs.

3422). Cells were trypsinized, resuspended in serum-free medium, and seeded into the upper chamber. The lower chamber was filled with medium containing 15% FBS as a chemoattractant. After 12 hours of incubation at 37°C with 5% CO_2, non-migrating cells on the upper surface of the membrane were removed with a cotton swab. Migrated cells on the lower surface were fixed, stained with crystal violet, and counted in five randomly selected fields per well under a microscope.

Scratch wound healing assay

Cells were seeded into 24-well plates and grown to confluence. A uniform scratch was created across the cell monolayer using a sterile pipette tip. After gently washing the wells with phosphate-buffered saline (PBS) to remove detached cells, images of the scratch were captured at 0, 24, and 48 hours using a microscope. The migration rate was calculated by measuring the change in scratch width over time with ImageJ software.

Western blot analysis

Cells in the logarithmic growth phase were lysed using radioimmunoprecipitation assay buffer containing protease inhibitors. Protein concentrations were determined with a bicinchoninic acid assay kit. Equal amounts of protein were separated by sodium dodecyl sulfate-polyacrylamide gel electrophoresis and transferred to polyvinylidene fluoride membranes. After blocking, the membranes were incubated overnight at 4°C with the following primary antibodies: anti-TLR4 (1:800, Cat# ab13556, Abcam, USA), anti-MyD88 (1:1000, Cat# ab2064, Abcam, USA), anti-Foxp3 (1:800, Cat # 12653, Cell Signaling Technology, USA), anti-IL-10 (1:800, Cat# ab133575, Abcam, USA), anti-IL-21 (1:800, Cat# ab125337, Abcam, USA), anti-TGF-β (1:800, Cat# ab215715, Abcam, USA), and anti-β-actin (1:10000, Cat# ab8227, Abcam, USA). After washing, the membranes were incubated with corresponding horseradish peroxidase-conjugated secondary antibodies (anti-rabbit or anti-mouse, Jackson ImmunoResearch) for 1 hour at room temperature. Protein bands were visualized using a chemiluminescent substrate and a gel imaging system. Glyceraldehyde-3-phosphate dehydrogenase functioned as the loading control. Relative protein expression levels were quantified employing ImageJ software.

Polymerase Chain Reaction (PCR) detection

Total RNA was extracted from cells or tissues using Trizol reagent. Complementary DNA was synthesized by reverse transcription. Quantitative PCR was performed using SYBR Green Master Mix on a real-time PCR system with the following conditions: initial denaturation at 95°C for 5 minutes; 40 cycles of 95°C for 30 seconds, 56°C for 30 seconds, and 72°C for 30 seconds; followed by a final extension at 72°C for 10 minutes. The sequences of the primers used are listed in **Table 1**. Gene expression levels were calculated using the $2^{(-\Delta\Delta Ct)}$ method, normalized to glyceraldehyde-3-phosphate dehydrogenase.

Animal experiments

Forty female C57BL/6 mice (for MB49 model) and C3H/He mice (for MBT-2 model), aged 6

weeks and weighing 17±1 g, were purchased from Shanghai Linghang Biotechnology Co., Ltd. (Production License SCXK (Shanghai) 2018-0003). MBT-2 and MB49 cells were cultured in medium containing 10% FBS and 100 U/mL penicillin-streptomycin under standard conditions. Upon reaching confluence, cells were trypsinized, washed with PBS, and prepared as a single-cell suspension at a density of 1×10^8 cells/mL. A 0.1 mL aliquot of the suspension was subcutaneously injected into the right axilla of each mouse. Tumor growth was monitored daily. Starting on day 7 post-inoculation, tumor size was measured by calipering the long and short diameters, and tumor volume was calculated.

To minimize animal suffering, all procedures were performed under general anesthesia induced with isoflurane. Post-operative analgesia was administered. At the experimental endpoint, mice were euthanized by CO_2 inhalation followed by cervical dislocation, in compliance with the approved animal protocol. The study protocol was reviewed and approved by the Animal Ethics Committee of Tianjin Medical University (Approval No.: TMUaMEC 20241001).

Detection of $CD4^+CXCR5^+PD\text{-}1^+$ Tfh and $CD4^+CXCR5^+FOXP3^+$ Tfr cells in mouse spleen

Single-cell suspensions were prepared from homogenized spleen tissue. For surface marker staining, cells were incubated with the following antibody cocktail at 4°C in the dark for 30 minutes: Fluorescein Isothiocyanate anti-mouse CD4 (Clone GK1.5, Cat# 100433, BioLegend, San Diego, CA, USA), phycoerythrin anti-mouse CXCR5 (Clone L138D7, Cat# 145506, BioLegend), and allophycocyanin anti-mouse PD-1 (Clone 29F.1A12, Cat# 135209, BioLegend). Cells were then washed with fluorescence-activated cell sorting buffer (phosphate-buffered saline containing 2% FBS). For intracellular staining of Foxp3, cells were fixed and permeabilized using the Foxp3/Transcription Factor Staining Buffer Set (Cat# 00-5523-00, eBioscience, Thermo Fisher Scientific, USA) according to the manufacturer's instructions, followed by incubation with peridinin-chlorophyll-protein-cyanine5.5 anti-mouse Foxp3 (Clone FJK-16s, Cat# 45-5773-82, eBioscience) at room temperature in the dark for 30 minutes. After a final wash, cells were resuspended in fluorescence-activated cell sorting buffer and analyzed on a flow cytometer (e.g., BD FACSCanto II). Data was analyzed using FlowJo software (Tree Star, Ashland, OR, USA). Tfh cells were defined as $CD4^+CXCR5^+PD\text{-}1^+$, and Tfr cells were defined as $CD4^+CXCR5^+Foxp3^+$.

Human tissue samples

Paired specimens of BCa and adjacent normal bladder tissue were obtained from patients who underwent surgery at Quzhou People's Hospital. The inclusion criteria were: (1) histologically confirmed primary BCa; (2) treatment with radical or partial cystectomy at the institution; and (3) no prior radiotherapy or chemotherapy before surgery. The exclusion criteria were: (1) presence of other synchronous malignancies; (2) history of autoimmune diseases or chronic infections; and (3) incomplete clinical or follow-up data. This study was approved by the Ethics Committee of Quzhou People's Hospital (Approval No. 202403012). Written informed consent was obtained from all participants. The study included patients with newly diagnosed BCa who had not received any prior medical intervention for this condition. For RNA extraction, all freshly collected tissue samples were instantly freshly collected in liquid nitrogen. Relevant clinical and pathologic data, including age, Tumor, Node, and Metastasis stage, tumor size, and lymph node involvement, were retrieved from patient medical records.

Statistical analysis

Data were presented as mean ± standard deviation from at least three independent experiments. Comparisons between two groups were performed using the two-tailed Student's t-test. Comparisons among more than two groups were analyzed by one-way analysis of variance followed by Tukey's post hoc test. For data involving multiple time points (e.g., tumor growth curve), two-way analysis of variance with Bonferroni post-test was used. The correlation between TLR4 expression and clinicopathologic features was analyzed using the Chi-square test or Fisher's exact test. Survival analysis was performed using the Kaplan-Meier method with the log-rank test. A p-value < 0.05 was considered significant. All analyses were conducted using SPSS 22.0

Table 2. Correlation between clinicopathologic characteristics and TLR4 expression in tumor tissues (n=206)

Characteristic	Total (n=206)	TLR4 Expression		*P* value
		Low (n=101)	High (n=105)	
Age (Years)				0.772
< 70	119	57 (27.6%)	59 (28.6%)	
≥ 70	87	44 (21.4%)	46 (22.4%)	
Gender				0.759
Male	169	80 (38.8%)	89 (43.2%)	
Female	37	21 (10.2%)	16 (7.8%)	
Pathologic Stage				0.048*
Stage I-II	148	79 (52.0%)	69 (48.0%)	
Stage III-IV	58	22 (37.9%)	36 (62.1%)	
T Stage				0.039*
T1-2	156	82 (52.6%)	74 (47.4%)	
T3-4	50	19 (38.0%)	31 (62.0%)	
N Stage				0.032*
N0	179	94 (52.5%)	85 (47.5%)	
N+ (N1&N2)	27	7 (25.9%)	20 (74.1%)	
Pathologic Grade				0.021*
Low grade	113	44 (38.9%)	69 (61.1%)	
High grade	93	57 (61.3%)	36 (38.7%)	

Abbreviations: TLR4, Toll-like receptor 4; T, Tumor; N, Node; M, Metastasis. Data are presented as number (percentage). Statistical significance was determined using the Chi-square test or Fisher's exact test, as appropriate. *P < 0.05.

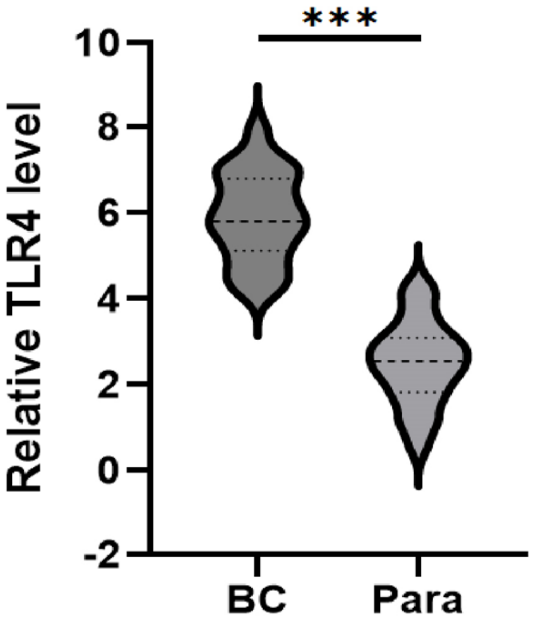

Figure 1. Comparative analysis of TLR4 expression levels between bladder tumor tissues and adjacent non-cancerous tissues. Abbreviations: TLR4, Toll-like receptor 4; BC, Bladder cancer; Para, Para-cancerous tissue. Data are presented as mean ± standard deviation. Statistical significance was determined using an unpaired, two-tailed Student's t-test. ***P < 0.001.

(IBM) and GraphPad Prism 9.0 (GraphPad Software).

Results

Upregulation of TLR4 expression in BCa

The TLR4 signaling pathway plays a crucial role in tumorigenesis. To investigate its involvement in BCa, we analyzed clinical samples and records from 206 patients. qPCR analysis revealed that TLR4 expression levels were significantly associated with tumor pathologic stage, Tumor, Node, Metastasis, and pathologic grade (**Table 2**). Furthermore, compared to adjacent non-cancerous tissues, bladder tumor tissues exhibited substantially higher TLR4 expression (**Figure 1**). These findings emphasized a strong correlation between elevated TLR4 expression and the initiation and progression of BCa.

Activation of TLR4 signaling pathway in BCa cell lines

To study the regulatory relationship between LPS and TLR4 signaling, we initially screened

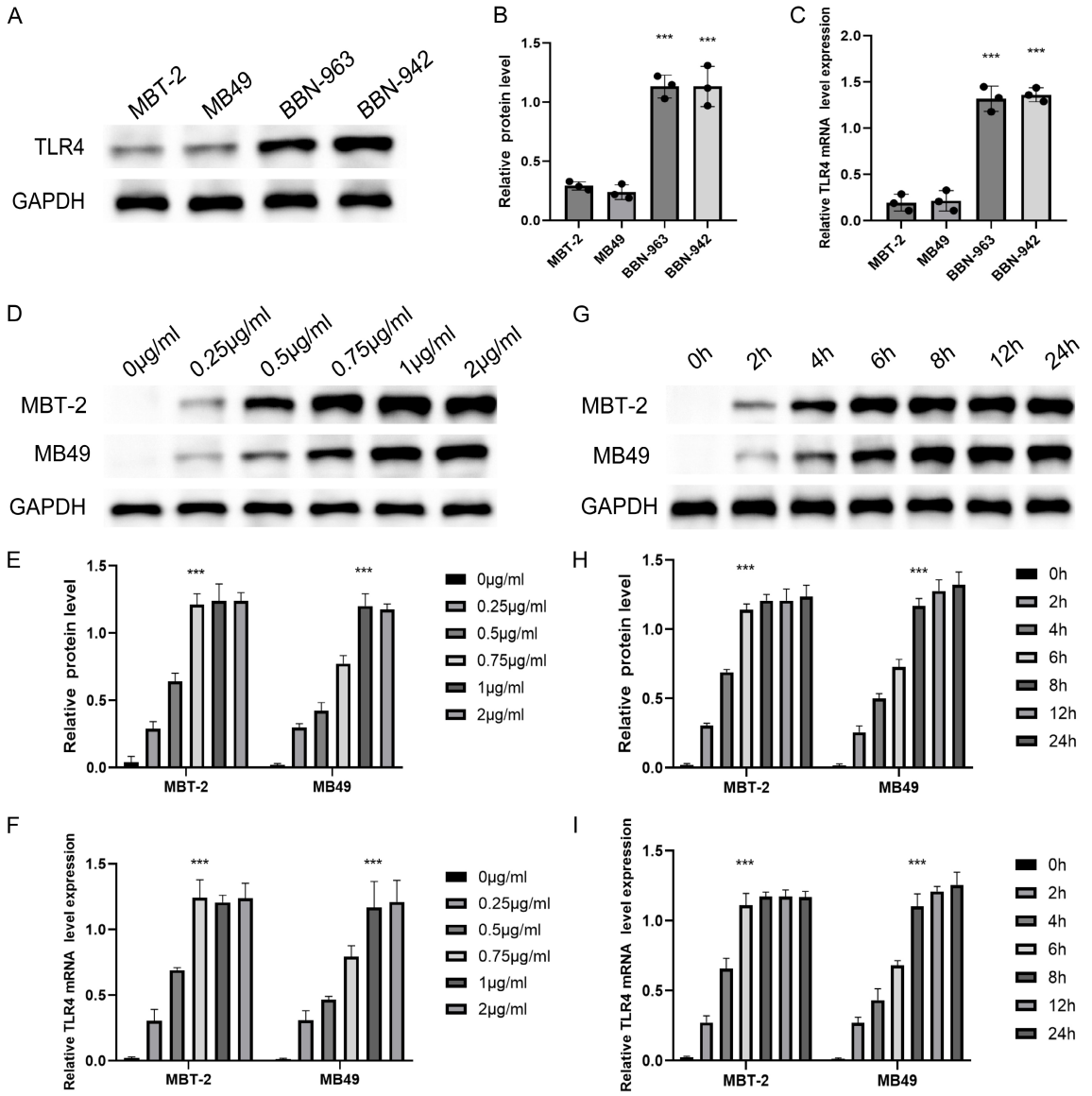

Figure 2. Activation of TLR4 signaling pathway in bladder cancer cell lines. (A, B) Protein expression levels of TLR4 in four bladder cancer cell lines (MBT-2, MB49, 5637, T24). (C) mRNA transcription levels of TLR4 in the same cell lines. (D, E) Protein expression levels of TLR4 in MBT-2 and MB49 cells after co-culture with varying concentrations of LPS (0, 0.25, 0.5, 0.75, 1.0, 2.0 μg/mL). (F) mRNA transcription levels of TLR4 under the same LPS concentration gradient. (G, H) Protein expression levels of TLR4 at different time points (0, 2, 4, 6, 8, 12 h) after co-culturing MBT-2 and MB49 cells with their respective optimal LPS concentrations (0.75 μg/mL for MBT-2, 1.0 μg/mL for MB49). (I) mRNA transcription levels of TLR4 at different time points. Abbreviations: TLR4, Toll-like receptor 4; mRNA, Messenger RNA; LPS, Lipopolysaccharide; ANOVA, Analysis of variance; GAPDH, Glyceraldehyde-3-phosphate dehydrogenase; BBN-963, N-Butyl-N-(4-hydroxybutyl)nitrosamine-963; BBN-942, N-Butyl-N-(4-hydroxybutyl)nitrosamine-942. Data are presented as mean ± standard deviation from three independent experiments. Statistical analysis was performed using one-way ANOVA followed by Tukey's post hoc test. All comparisons are made against the 0 μg/mL group (D-F) or the 0 h time point (G-I). ***P < 0.001.

four BCa cell lines: MBT-2, MB49, 5637, and T24. mRNA and protein analyses showed relatively low basal TLR4 expression in MBT-2 and MB49 cells (**Figure 2A-C**). We therefore selected these two lines for subsequent experiments. Cells were treated with a range of LPS concentrations (0, 0.25, 0.5, 0.75, 1.0, 2.0 μg/mL) for 24 hours. TLR4 expression peaked at 0.75 μg/mL LPS in MBT-2 cells and at 1.0 μg/mL in MB49 cells (**Figure 2D-F**). A time-

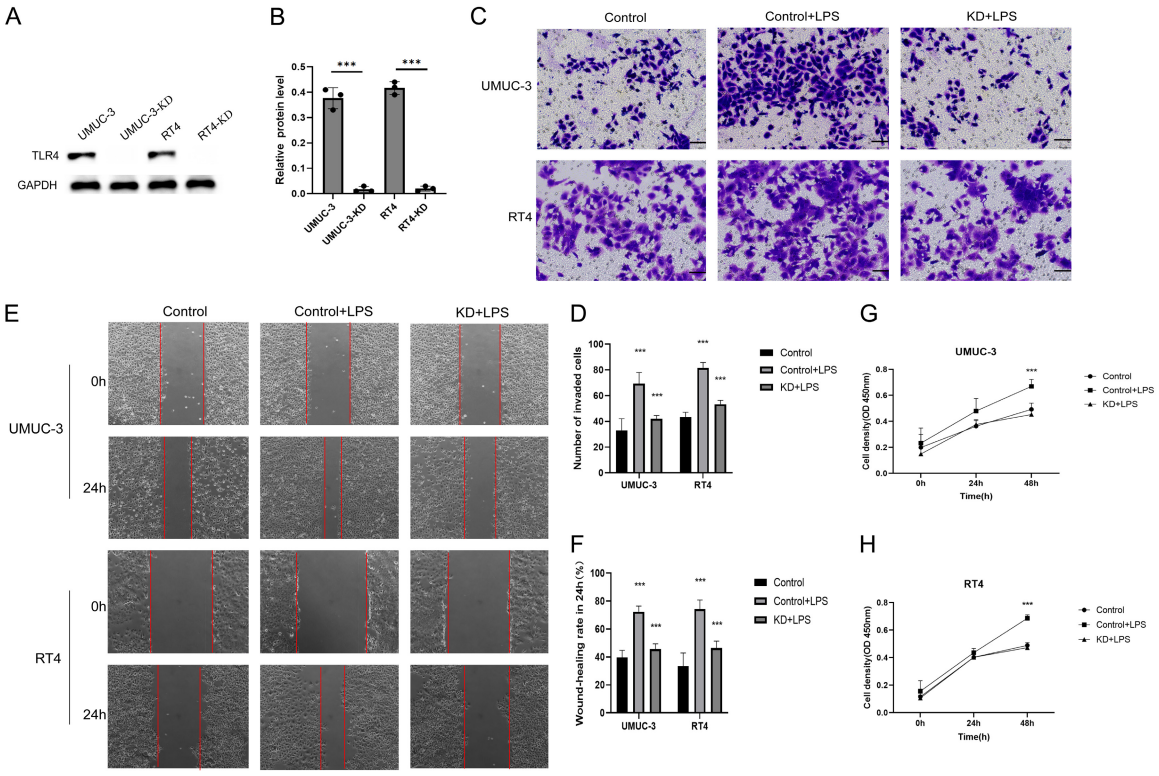

Figure 3. *In vitro* study on the regulatory role of TLR4 in bladder cancer. (A, B) Protein expression levels of TLR4 in MBT-2 and MB49 cell lines after stable TLR4-KD. (C, D) Transwell migration assay results for both cell lines under different treatment conditions: Control, Control+LPS, and KD+LPS. (E, F) Scratch wound healing assay results for both cell lines under the same three treatment conditions. (G, H) MTT cell proliferation assay results over time (0, 24, 48 h) under the same three treatment conditions. Abbreviations: TLR4, Toll-like receptor 4; GAPDH, Glyceraldehyde-3-phosphate dehydrogenase; KD, Knockdown; LPS, Lipopolysaccharide; ANOVA, Analysis of variance; MTT, 3-(4,5-Dimethylthiazol-2-yl)-2,5-diphenyltetrazolium bromide. Data are presented as mean ± standard deviation from three independent experiments. For (A-F), statistical significance was determined by one-way ANOVA with Tukey's post hoc test. For (G, H), two-way ANOVA with Bonferroni's post-test was used. ***P < 0.001.

course experiment using these optimal concentrations revealed that TLR4 expression in MBT-2 cells peaked after 6 hours of treatment, while in MB49 cells it peaked at 8 hours (**Figure 2G-I**).

In vitro study on the regulatory role of TLR4 in BCa

To determine whether the regulatory effects of LPS depend on TLR4, we established stable TLR4-KD cell lines (MBT-2-KD-TLR4 and MB49-KD-TLR4; **Figure 3A**, **3B**). Functional assays demonstrated that LPS treatment significantly enhanced the invasive capacity of both wild-type cell lines in Transwell assays, an effect that was completely abolished in the TLR4-KD cells (**Figure 3C**, **3D**). Similarly, the scratch wound healing assay showed that LPS markedly increased the migratory capacity of control cells after 24 hours, which was substantially reduced upon TLR4-KD (**Figure 3E**, **3F**). The MTT assay confirmed that LPS promoted cell proliferation in control cells, whereas the proliferative advantage was lost in the KD+LPS groups over a 48-h period (**Figure 3G**, **3H**). Collectively, these *in vitro* results indicated that LPS exerts significant pro-tumorigenic effects primarily through the activation of the TLR4 signaling pathway.

In vivo study on the regulatory role of TLR4 in BCa

We next evaluated the role of TLR4 in a subcutaneous xenograft model using C57BL/6 mice (for MB49) and C3H/He mice (for MBT-2). Tumors formed from control cells treated with LPS (Control+LPS group) exhibited significantly higher growth rates as well as larger final vol-

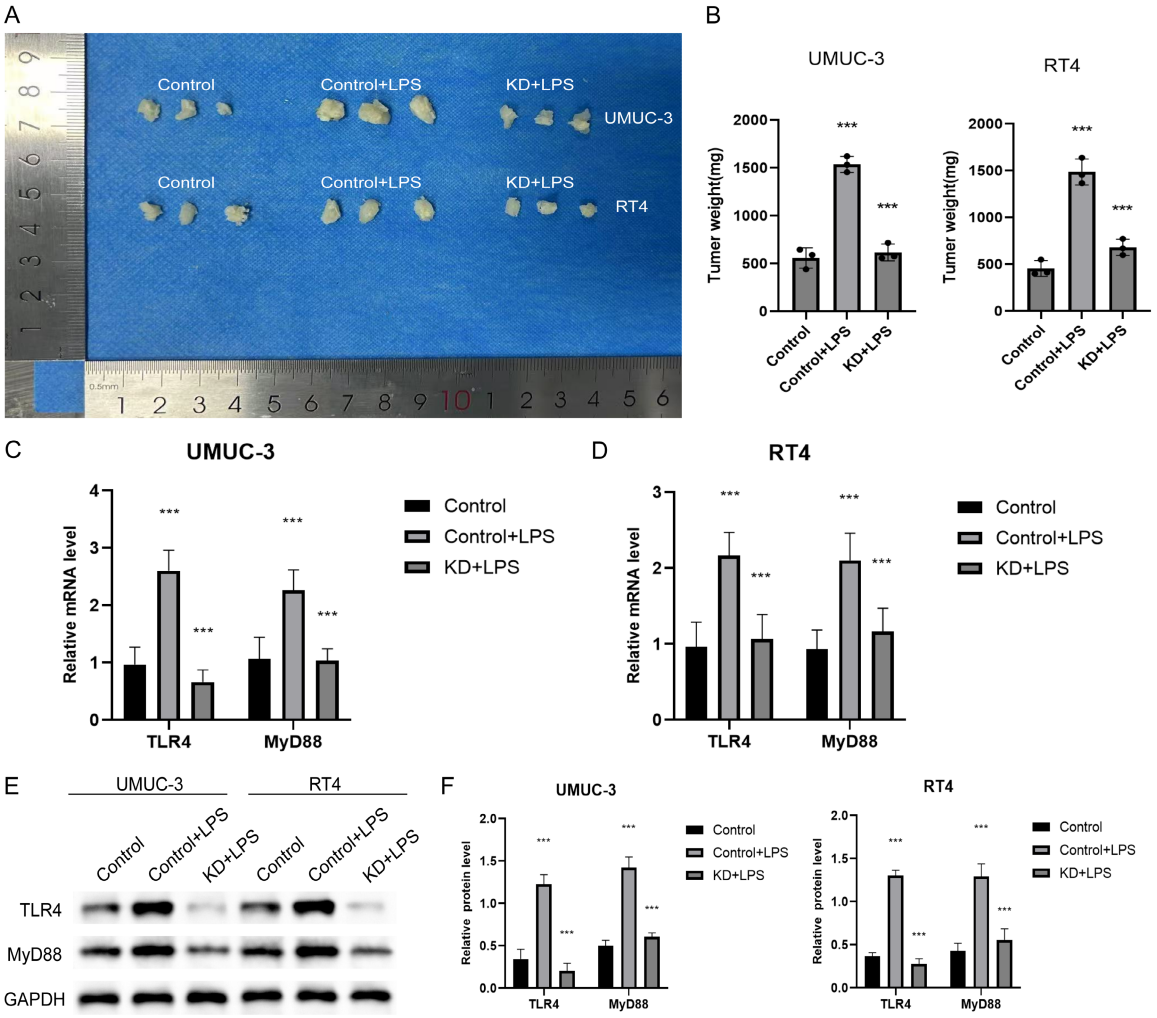

Figure 4. *In vivo* study on the regulatory role of TLR4 in bladder cancer. (A, B) Subcutaneous tumor growth curves in C57BL/6 mice injected with MB49 cells and C3H/He mice injected with MBT-2 cells from different groups: Control, Control+LPS, and KD+LPS. Tumor volume was measured over time. (C, D) mRNA expression levels of TLR4 and MyD88 in tumor tissues harvested from the different treatment groups. (E, F) Protein expression levels of TLR4 and MyD88 in the same tumor tissues. Abbreviations: TLR4, Toll-like receptor 4; LPS, Lipopolysaccharide; KD, Knockdown; GAPDH, Glyceraldehyde-3-phosphate dehydrogenase; ANOVA, Analysis of variance; MyD88, Myeloid differentiation primary response 88. Data are presented as mean ± standard deviation (n ≥ 5 mice per group). For tumor growth curves (A, B), statistical analysis was performed using two-way ANOVA with Bonferroni's post-test. For gene and protein expression (C-F), one-way ANOVA with Tukey's *post hoc* test was used. ***P < 0.001.

umes compared to the Control group. In contrast, tumors derived from TLR4-KD cells (KD+LPS group) showed a significant reduction in growth and volume compared to the Control+LPS group (**Figure 4A**, **4B**). Analysis of tumor tissues revealed that mRNA levels of TLR4 and MyD88 were significantly upregulated in the Control+LPS group but markedly decreased in the KD+LPS group (**Figure 4C**, **4D**). Western blot analysis of the same tissues confirmed these trends at the protein level (**Figure 4E**, **4F**).

Molecular mechanisms of LPS-mediated TLR4 regulation in BCa

Given the established link between TLR4 and immune evasion, we investigated whether LPS remodels the TIME. Flow cytometric analysis of splenocytes from tumor-bearing mice revealed that the LPS-treated group had a significantly increased number of Tfh cells and fewer Tfr cells. This discovery led to a markedly elevated Tfh/Tfr ratio. This imbalance was corrected in the KD+LPS group (**Figure 5A**, **5B**). Furthermore,

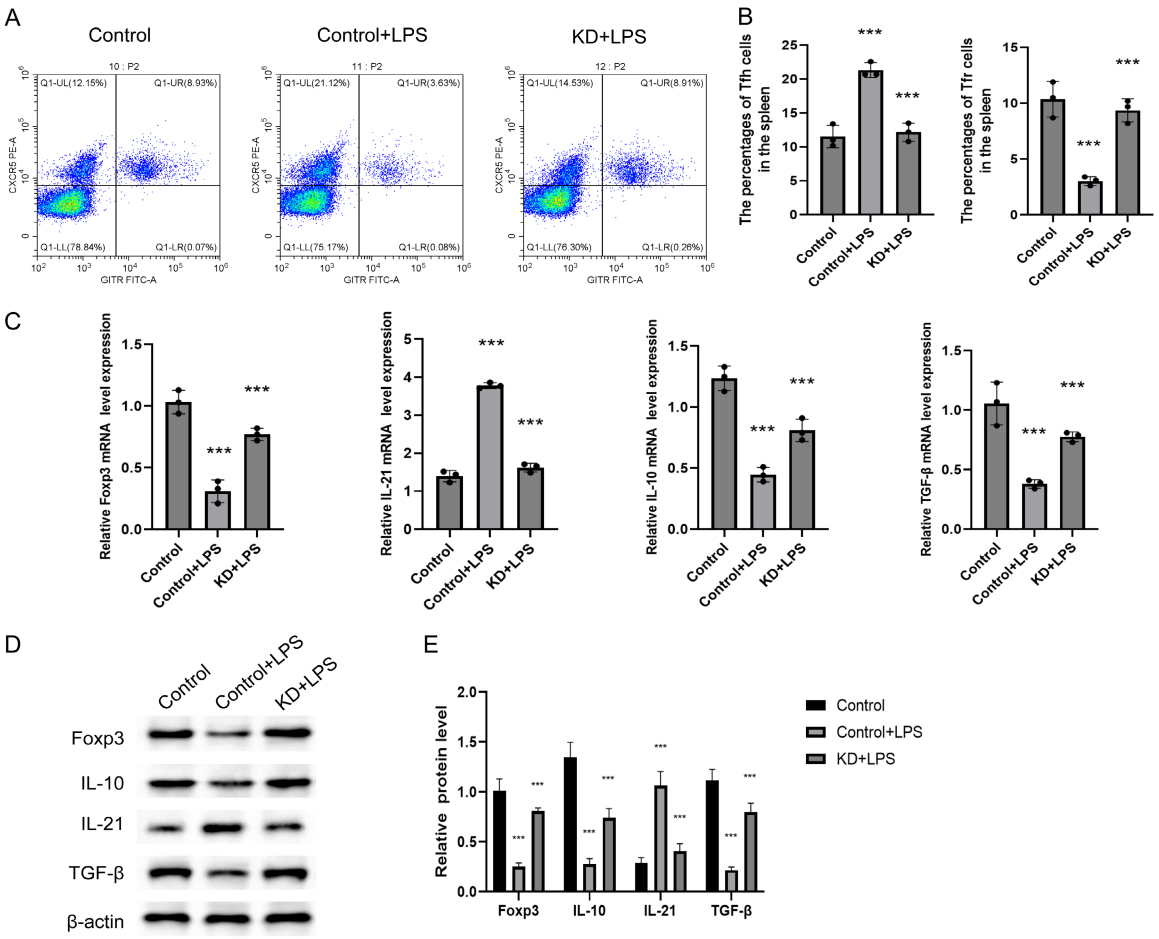

Figure 5. Molecular mechanisms of LPS-mediated TLR4 regulation in bladder cancer. (A, B) Flow cytometry analysis of Tfh and Tfr cells in the spleens of MBT-2 tumor-bearing mice from different groups. Representative flow plots (A) and quantification of the Tfh/Tfr ratio (B) are shown. (C) Relative mRNA expression levels of Foxp3, IL-21, IL-10, and TGF-β in tumor tissues. (D, E) Western blot analysis and quantification of protein expression levels of Foxp3, IL-21, IL-10, and TGF-β in tumor tissues. Abbreviations: TLR4, Toll-like receptor 4; LPS, Lipopolysaccharide; KD, Knockdown; Tfh cells, T follicular helper cells; Tfr cells, T follicular regulatory cells; Foxp3, Forkhead box P3; IL-21, Interleukin-21; IL-10, Interleukin-10; TG-β: Transforming growth factor-beta; ANOVA, Analysis of variance. Data are presented as mean ± standard deviation (n ≥ 5 mice per group for in vivo experiments; three independent replicates for in vitro assays). Statistical analysis was performed using one-way ANOVA with Tukey's *post hoc* test. ***P < 0.001.

reverse transcription-qPCR analysis of tumor tissues showed that LPS treatment decreased mRNA levels of Foxp3, IL-10, and TGF-β, while increasing IL-21 expression. TLR4-KD reversed these cytokine expression changes (**Figure 5C**). Western blot analysis of the corresponding proteins corroborated these findings (**Figure 5D**, **5E**).

Discussion

This study elucidates a novel mechanism by which LPS promotes BCa progression. We demonstrate that LPS activates the TLR4/MyD88 signaling pathway in tumor cells, which accomplishes two key pro-tumorigenic functions: it directly accelerates cancer cell growth and spread, and it systemically disrupts immune homeostasis by skewing the balance between Tfh and Tfr cells. This dual action collectively fosters an immunosuppressive niche. Our findings provide a new perspective for understanding BCa progression through the lens of infection-mediated immune dysregulation.

The role of TLR4 in cancer is context-dependent and complex. While its activation on immune cells can initiate protective anti-tumor responses [11-13], aberrant signaling within tumor cells themselves often promotes malignancy. For

instance, TLR4 activation has been shown to facilitate immune evasion and metastasis in liver and colon cancers [14-16]. Our research confirms and extends this paradigm to BCa. We found that LPS stimulation, acting through TLR4, enhances the aggressive behavior of BCa cells *in vitro* and *in vivo*. Critically, clinical correlation analysis revealed that higher TLR4 expression in patient tumors is associated with more advanced disease stage and lymph node metastasis, underscoring its likely role in clinical progression. Our work solidly identifies TLR4 as a culpable "accomplice" in BCa pathogenesis, delineating a specific LPS-TLR4-MyD88 axis.

The most significant novelty of our study lies in connecting TLR4 signaling to the precise immunological rheostat of the Tfh/Tfr equilibrium. Tfh cells function as an "accelerator" for humoral immunity by supporting B-cell activity, whereas Tfr cells act as the essential "brakes" that express Foxp3 to suppress excessive Tfh-driven responses and maintain immune homeostasis [17-19]. How this balance is perturbed in BCa was previously unclear. Our data provides a clear mechanistic answer: LPS, acting through TLR4, tilts this balance decisively toward Tfh cells. This shift is accompanied by a characteristic cytokine profile change, marked by increased levels of the pro-inflammatory and Tfh-associated cytokine IL-21, alongside decreased expression of the suppressive molecules Foxp3, IL-10, and TGF-β. This state resembles an immune system with its accelerator engaged while its brakes are failing, creating a dysregulated, pro-tumor immune environment [20]. To our knowledge, this is the first report to identify the LPS-TLR4 axis as the upstream disruptor of the Tfh/Tfr balance in BCa.

From a translational standpoint, our findings have important implications. First, they offer a plausible explanation for the poorer outcomes often observed in BCa patients with recurrent urinary tract infections, which are frequently caused by LPS-producing bacteria like *Escherichia coli*. Chronic LPS exposure could, through the mechanism we describe, progressively impair the peri-tumoral immune environment, foster tumor growth, and diminish the efficacy of immunotherapies like BCG. Second, our work highlights new therapeutic avenues. Targeting the TLR4 signaling pathway with specific inhibitors could emerge as promising approaches. The feasibility of modulating this pathway for therapeutic benefit is supported by interventions in other LPS-driven diseases. For instance, natural compounds have been shown to alleviate tissue injury by specifically blocking the TLR4/MyD88/NF-κB pathway [21], providing a proof-of-concept for pharmacologic intervention at this nodal point. Alternatively, developing strategies to recalibrate the Tfh/Tfr balance represents another promising direction. Combining a TLR4 antagonist with intravesical BCG therapy might yield synergistic benefits by simultaneously attacking tumor cells and rectifying the immunosuppressive microenvironment.

We acknowledge several limitations of our study. While our models provide strong mechanistic evidence, the conclusions are derived primarily from cell lines and mouse studies, whereas the human tumor microenvironment is more complex. Therefore, future work should directly validate the correlation between TLR4 levels and Tfh/Tfr cell dynamics in a larger cohort of primary human BCa specimens. In addition, although we established the TLR4-MyD88 axis as critical, the specific downstream signaling nodes (e.g., NF-κB, MAPK pathways) that execute these cellular and immunological changes warrant deeper investigation. Third, our *in vivo* immune analysis focused on the spleen; future studies should also examine the status of Tfh and Tfr cells within the tumor microenvironment and tumor-draining lymph nodes to provide a more comprehensive spatial understanding.

In conclusion, our research demonstrates that LPS, by activating TLR4 on BCa cells, acts as a dual-acting driver of malignancy. It directly fuels tumor growth and, concurrently, disrupts systemic immune homeostasis by specifically impairing the coordinated interplay between Tfh and Tfr cells. This work establishes a foundation for understanding BCa progression through the "infection-immunity-tumor" axis and provides a rational basis for future therapies targeting either the TLR4 pathway or the Tfh/Tfr equilibrium.

Disclosure of conflict of interest

None.

Address correspondence to: Lijun Wan, Department of Urology, The Quzhou Affiliated Hospital of Wenzhou Medical University, Quzhou People's Hospital, 100 Minjiang Avenue, Kecheng District, Quzhou 324000, Zhejiang, China. Tel: +86-18622645876; E-mail: Lijunwan2025@163.com

References

[1] Tittarelli A, González FE, Pereda C, Mora G, Muñoz L, Saffie C, García T, Díaz D, Falcón C, Hermoso M, López MN and Salazar-Onfray F. Toll-like receptor 4 gene polymorphism influences dendritic cell in vitro function and clinical outcomes in vaccinated melanoma patients. Cancer Immunol Immunother 2012; 61: 2067-2077.

[2] Rajaiah R, Perkins DJ, Ireland DD and Vogel SN. CD14 dependence of TLR4 endocytosis and TRIF signaling displays ligand specificity and is dissociable in endotoxin tolerance. Proc Natl Acad Sci U S A 2015; 112: 8391-8396.

[3] Bardoli AD, Afshar M, Viney R, Foster M, Porfiri E, Zarkar A, Stevenson R, James ND, Bryan RT and Patel P. The PD-1/PD-L1 axis in the pathogenesis of urothelial bladder cancer and evaluating its potential as a therapeutic target. Future Oncol 2016; 12: 595-600.

[4] Wang L, Qian J, Lu Y, Li H, Bao H, He D, Liu Z, Zheng Y, He J, Li Y, Neelapu S, Yang J, Kwak LW, Yi Q and Cai Z. Immune evasion of mantle cell lymphoma: expression of B7-H1 leads to inhibited T-cell response to and killing of tumor cells. Haematologica 2013; 98: 1458-1466.

[5] Rosborough BR, Raïch-Regué D, Matta BM, Lee K, Gan B, DePinho RA, Hackstein H, Boothby M, Turnquist HR and Thomson AW. Murine dendritic cell rapamycin-resistant and rictor-independent mTOR controls IL-10, B7-H1, and regulatory T-cell induction. Blood 2013; 121: 3619-3630.

[6] Huang X, Chen Y, Chung CS, Yuan Z, Monaghan SF, Wang F and Ayala A. Identification of B7-H1 as a novel mediator of the innate immune/proinflammatory response as well as a possible myeloid cell prognostic biomarker in sepsis. J Immunol 2014; 192: 1091-1099.

[7] Huang B, Zhao J, Li H, He KL, Chen Y, Chen SH, Mayer L, Unkeless JC and Xiong H. Toll-like receptors on tumor cells facilitate evasion of immune surveillance. Cancer Res 2005; 65: 5009-5014.

[8] Takeda K, Kaisho T and Akira S. Toll-like receptors. Annu Rev Immunol 2003; 21: 335-376.

[9] Ma J, Usui Y, Kezuka T, Okunuki Y, Zhang L, An X, Mizota A and Goto H. Costimulatory molecule expression on human uveal melanoma cells: functional analysis of CD40 and B7-H1. Exp Eye Res 2012; 96: 98-106.

[10] Tang X and Zhu Y. TLR4 signaling promotes immune escape of human colon cancer cells by inducing immunosuppressive cytokines and apoptosis resistance. Oncol Res 2012; 20: 15-24.

[11] Meng L, Li L, Lu S, Li K, Su Z, Wang Y, Fan X, Li X and Zhao G. The protective effect of dexmedetomidine on LPS-induced acute lung injury through the HMGB1-mediated TLR4/NF-κB and PI3K/Akt/mTOR pathways. Mol Immunol 2018; 94: 7-17.

[12] Zhang C, Wang X, Wang C, He C, Ma Q, Li J, Wang W, Xu YT and Wang T. Qingwenzhike prescription alleviates acute lung injury induced by LPS via inhibiting TLR4/NF-kB pathway and NLRP3 inflammasome activation. Front Pharmacol 2021; 12: 790072.

[13] Liu Y, Zhou J, Luo Y, Li J, Shang L, Zhou F and Yang S. Honokiol alleviates LPS-induced acute lung injury by inhibiting NLRP3 inflammasome-mediated pyroptosis via Nrf2 activation in vitro and in vivo. Chin Med 2021; 16: 127.

[14] Rosadini CV and Kagan JC. Early innate immune responses to bacterial LPS. Curr Opin Immunol 2017; 44: 14-19.

[15] Fu J and Wu H. Structural mechanisms of NLRP3 inflammasome assembly and activation. Annu Rev Immunol 2023; 41: 301-316.

[16] Zhou L, Liu Z, Wang Z, Yu S, Long T, Zhou X and Bao Y. Astragalus polysaccharides exerts immunomodulatory effects via TLR4-mediated MyD88-dependent signaling pathway in vitro and in vivo. Sci Rep 2017; 7: 44822.

[17] Mallampalli RK, Kaercher L, Snavely C, Pulijala R, Chen BB, Coon T, Zhao J and Agassandian M. Fbxl12 triggers G1 arrest by mediating degradation of calmodulin kinase I. Cell Signal 2013; 25: 2047-2059.

[18] Uboha NV, Flajolet M, Nairn AC and Picciotto MR. A calcium- and calmodulin-dependent kinase Ialpha/microtubule affinity regulating kinase 2 signaling cascade mediates calcium-dependent neurite outgrowth. J Neurosci 2007; 27: 4413-4423.

[19] Mito T, Vincent AE, Faitg J, Taylor RW, Khan NA, McWilliams TG and Suomalainen A. Mosaic dysfunction of mitophagy in mitochondrial muscle disease. Cell Metab 2022; 34: 197-208, e195.

[20] Palikaras K, Lionaki E and Tavernarakis N. Mechanisms of mitophagy in cellular homeostasis, physiology and pathology. Nat Cell Biol 2018; 20: 1013-1022.

[21] Xu k, Xiang Y and Fang SP. A review on angelica sinensis alleviates acute lungtissue injury through TLR-4/MyD88 signal pathway. Perioper Precis Med 2024; 2: 124-131.